European Radiology (2019) 29:1831–1840
https://doi.org/10.1007/s00330-018-5728-0

MUSCULOSKELETAL

Comparison of the diagnostic performance of CT Hounsfield unit histogram analysis and dual-energy X-ray absorptiometry in predicting osteoporosis of the femur

Hyun Kyung Lim[1] · Hong Il Ha[2] · Sun-Young Park[2] · Kwanseop Lee[2]

Received: 15 May 2018 / Revised: 31 July 2018 / Accepted: 27 August 2018 / Published online: 25 September 2018

Abstract

Purpose To evaluate the diagnostic performance of Hounsfield unit histogram analysis (HUHA) of precontrast abdominal-pelvic CT scans for predicting osteoporosis.

Materials and methods The study included 271 patients who had undergone dual X-ray absorptiometry (DXA) and abdominal-pelvic CT within 1 month. HUHA was measured using commercial 3D analysis software (Aquarius iNtuition v4.4.12®, TeraRecon) and expressed as a percentage of seven HU range categories related to the ROI: A < 0, 0 ≤ B < 25, 25 ≤ C < 50, 50 ≤ D < 75, 75 ≤ E < 100, 100 ≤ F < 130, and 130 ≤ G. A coronal reformatted precontrast CT image containing the largest Ward's triangle was selected and then the ROI was drawn over the femoral neck. Correlation (*r*) and ROC curve analyses were used to assess diagnostic performance in predicting osteoporosis using the femur *T*-score as the reference standard.

Results When the femur *T*-score was used as the reference, the *r*s of HUHA-A and HUHA-G were 0.74 and -0.57, respectively. Other HUHA values had moderate to weak correlations (r = -0.33 to 0.27). The correlation of HUHA-A was significantly higher than that of HUHA-G ($p = 0.03$). The area under the curve (0.95) of HUHA-A differed significantly from that of HUHA-G (0.90; $p < 0.01$). A HUHA-A threshold ≥ 27.7% was shown to predict osteoporosis based on a sensitivity and specificity of 95.6% and 81.7%, respectively.

Conclusion The HUHA-A value of the femoral neck is closely related to osteoporosis and may help predict osteoporosis.

Key Points

- *HUHA correlated strongly with the DXA femur T-score (HUHA-A, r = 0.74).*
- *The diagnostic performance of HUHA for predicting osteoporosis (AUC = 0.95) was better than that of the average CT HU value (AUC = 0.91; p < 0.05).*
- *HUHA may help predict osteoporosis and enable semi-quantitative measurement of changes in bone mineral density.*

Keywords Diagnosis, Computer-assisted · Osteoporosis · Tomography, X-ray computed · Absorptiometry, Photon

Abbreviations

ATCM	Automatic tube current modulation
ATVS	Automatic tube voltage selection
BMD	Bone mineral density
CI	Confidence interval
DXA	Dual-energy X-ray absorptiometry
HU	Hounsfield unit
HUHA	Hounsfield unit histogram analysis
ICC	Intra-class correlation coefficient

✉ Hong Il Ha
ha.hongil@gmail.com

[1] Department of Radiology, Soonchunhyang University Seoul Hospital, 59, Daesagwan-ro, Yongsan-gu, Seoul, Republic of Korea 04401

[2] Department of Radiology, Hallym University Sacred Heart Hospital, 22, Gwanpyeong-ro 170beon-gil, Dongan-gu, Anyang-si, Gyeonggi-do, Republic of Korea 14068

Introduction

As the elderly population grows, osteoporosis is considered a major public health concern [1]. Approximately 1.5 million of the fractures that occur annually in the United States are attributed to osteoporosis, and up to 50% of women and 20% of men are at risk of developing an osteoporosis-related fracture

during their life [2, 3]. Among the osteoporosis related-fractures, proximal femur fracture is one of most common complications and is associated with higher mortality and morbidity [4].

Dual-energy X-ray absorptiometry (DXA) is the standard method for diagnosing osteoporosis, as the WHO definition of osteoporosis is based on the DXA *T*-score. Osteoporosis is diagnosed using central DXA in postmenopausal women and men aged ≥ 50 years if the *T* -score of the lumbar spine or hip is -2.5 or less [5]. Although the revised and expanded recommendations of the U.S. Preventive Services Task Force emphasise the importance of more screening [6], DXA as a screening method is underused, and there is a growing appreciation of the need for broader screening efforts [7, 8].

More than 25 million abdominal-pelvic CT scans are performed on adults each year in the United States. Even if a small number of these patients undergo opportunistic osteoporosis screening, the impact could be substantial. Recently, several studies have shown optimistic results using CT for opportunistic screening of osteoporosis [9–14]. These reports showed that the average CT HU value for multiple or even a single vertebra is correlated with the DXA *T*-score and could be used for opportunistic screening of osteoporosis, providing several threshold cut-off values yielding a high specificity for identifying osteoporosis. However, these studies focused on the lumbar spine using average CT HU values [10, 12, 13, 15]. The diagnosis of osteoporosis is based on the *T*-score of the lumbar spine or femoral neck [5]. The femoral neck is an ideal site to assess osteoporosis, for several reasons. First, the femoral neck is unaffected by degenerative arthritis, unlike the lumbar spine [16]. Second, the femoral neck consists mainly of dense trabecular bones and Ward's triangle. Both are closely related to osteoporosis, since trabecular bone is especially affected by osteoporosis [17, 18]. Third, focal osteoporosis defects play an important role in hip fracture [17]. In addition, bone mineral density (BMD) of the femur is a strong predictor of hip fracture [19, 20].

As osteoporosis progresses, BMD decreases, and bony microstructure changes occur [18]. Change in the microstructure of trabecular bone is represented as a decrease in the HU value on CT. The HU histogram presents the distribution of variable HU values from fat tissue to hard cortical bone. The average HU value is a single value representative of certain ROIs but is a summation of the HU histogram. Thus, CT HU histogram analysis could be more important than the average CT HU value for assessing BMD changes during osteoporosis. The aim of this retrospective study was to evaluate the diagnostic performance of CT HU histogram analysis on precontrast abdominal-pelvic CT (APCT) scans in predicting osteoporosis in adults > 50 years of age, using the DXA *T*-score as the reference standard.

Materials and Methods

This retrospective study was approved by our institutional review board, and informed consent was waived.

Patients

Between March and July of 2017, 279 consecutive patients 50 years or older who underwent APCT and had undergone DXA within 30 days (mean 5.3 days, range 0–25 days) were included, retrospectively. Among them, eight patients were excluded due to bone metastasis (n = 6) and any total hip arthroplasty (n = 2). Finally, 271 patients (mean age 69.5 years, range 50–96 years) were included in the study cohort. This cohort comprised 47 men (mean age 69.5 years; range 50–90 years) and 224 women (mean age 69.5 years; range 50–96 years). The reasons for CT imaging were as follows: tumour metastasis surveillance (n = 157), minor trauma such as slip-down injury or simple fall-down injury (n = 80), and routine health check-up or medical inspection (n = 34) (Fig. 1). None of the 271 patients had any bone diseases. All 157 patients who underwent tumour metastasis surveillance were female breast cancer patients, none of whom had taken anticancer drugs for 3 months before the DXA and APCT.

DXA

DXA of the proximal femur for BMD assessment was performed using the standard technique according to the International Society for Clinical Densitometry guidelines using Lunar Prodigy densitometers® (GE Healthcare). The lowest DXA *T*-score of the femoral neck was used as the reference standard. The WHO definition of osteoporosis of

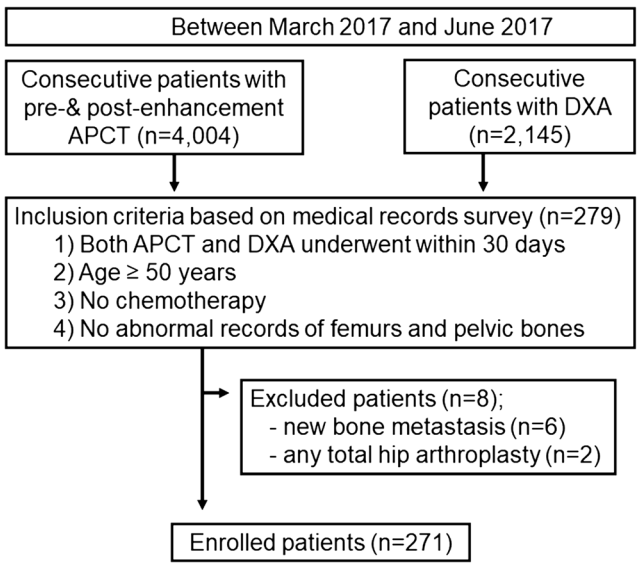

Fig. 1 Flowcharts of patient selection. APCT = abdominal-pelvic CT; DXA = dual-energy X-ray absorptiometry

the femur head is a DXA *T*-score ≤ -2.5. Osteopenia is defined as a DXA *T*-score of -1.0 to -2.4. A DXA *T*-score > -1.0 is defined as normal.

CT imaging

All CT examinations were performed using three multidetector-row CT (MDCT) scanners (SOMATOM SENSATION 64, SOMATOM Definition Edge, SOMATOM Definition Flash; Siemens Healthcare) in standard single-energy CT mode. Automatic tube voltage selection (ATVS; Care kVp) and automatic tube current modulation (ATCM; CARE Dose 4D) protocols were used with the SOMATOM Definition Edge and SOMATOM Definition Flash CT scanners. Only the ATCM protocol was used with the SOMATOM SENSATION 64 CT scanner. Although automated tube voltage selection chooses kVp values ranging from 80−140 kV, our study patients were examined at either 100 kVp or 120 kVp. With the patient in the supine position, both precontrast and contrast-enhanced CT images were obtained from the diaphragm to the pubic symphysis. A precontrast CT was performed first. Portal venous-phase imaging was conducted 50 s after an intravenous injection of 100–150 mL iodinated contrast material at a rate of 2.5−4 mL/s through the antecubital vein. However, to exclude the effect of the contrast agent on the CT Hounsfield unit measurement, all measurements were performed using only the precontrast CT images [21].

The scanning parameters of SOMATOM SENSATION 64 CT scans (n = 19) were as follows: detector collimations, 64 × 0.625 mm; pitch, 1.4; gantry rotation time, 0.5 s; tube current, 210 mAs; tube voltage, 120 kVp; and filter back projection with soft tissue kernel (B40f). The scanning parameters of SOMATOM Definition Edge and SOMATOM Definition Flash CT scans (n = 252) were as follows: detector collimations, 128 × 0.6 mm; pitch, 0.6; gantry rotation time, 0.5 s; tube current, 200 or 289 mAs; tube voltage, either 100 kVp (n = 93) or 120 kVp (n = 159); and Sinogram-Affirmed Iterative Reconstruction with soft tissue kernel (I40f) applied with S1 iteration level. The raw data were routinely reformatted in the axial and coronal planes based on a section thickness of 5 mm and an interval of 5 mm.

HUHA and average CT HU measurements

HUHA and average CT HU measurements were performed on coronal reformatted precontrast images (5 mm slice thickness) using commercial three-dimensional (3-D) analysis software (Aquarius iNtuition v4.4.12®, TeraRecon). All measurements from the 271 patients were performed by one radiologist (H.I.H). To assess interrater agreement, two radiologists (H.I.H. with 10 years of experience interpreting body images and S.Y.P. with 4 years of experience interpreting musculoskeletal images) measured the HUHA and average CT HU values in images from 30 randomly selected femoral neck cases. Interobserver reliability was estimated by one radiologist (H.I.H) at a 4-week interval to prevent recall bias. Prior to conducting the measurements, there was no specific interactive training session to learn the measurement techniques. Observers selected the image that contained the greatest amount of Ward's triangle and the principal compressive trabecula on the coronal reformatted image and then drew the largest ROI over the femoral neck and intertrochanteric area adjacent to the outer cortex. The HUHA is expressed as a percentage of the ROI and can be classified into seven arbitrarily determined categories, as follows: A < 0, 0 ≤ B < 25, 25 ≤ C < 50, 50 ≤ D < 75, 75 ≤ E < 100, 100 ≤ F < 130, and 130 ≤ G. The area of each HU range can be automatically calculated as a percentage of the entire area using the 3-D analysis software. This software displays the colours according to each HUHA range. The average HU value was simultaneously calculated using the same reformatted coronal image for the same ROIs (Fig. 2).

Statistical analysis

The patient cohort was divided into the osteoporosis and non-osteoporosis groups according to the femur *T*-score. Demographic variables, HUHA categories, and average CT HU values were expressed as means with standard deviations and compared using the independent *t*-test to determine differences between two groups.

Correlation analysis was used to determine the HUHA categories and average CT HU values that best reflect the femur *T*-score qualitatively. The significance of the correlation coefficients was measured by Z-test. Since covariance among HUHA variables is a possibility, simple linear regression analysis (r^2) was performed using the strongest variable from the correlation analysis.

The diagnostic performance of HUHA and the average CT HU value in predicting osteoporosis with respect to the femur *T*-score reference standard was evaluated by ROC curve analysis using those variables showing a high correlation in the simple linear regression analysis.

Intra-observer agreement in terms of HUHA and average CT HU measurements was assessed based on a two-way mixed intra-class correlation coefficient (ICC) with absolute agreement. An ICC > 0.75 was considered to represent good agreement [22, 23]. Interobserver agreement was calculated using the kappa statistic. Kappa values were interpreted according to the criteria of Landis and Koch [24]. Statistical analyses were performed using commercial software (MedCalc®, MedCalc Software bvba). A p value < 0.05 was considered to indicate a significant difference.

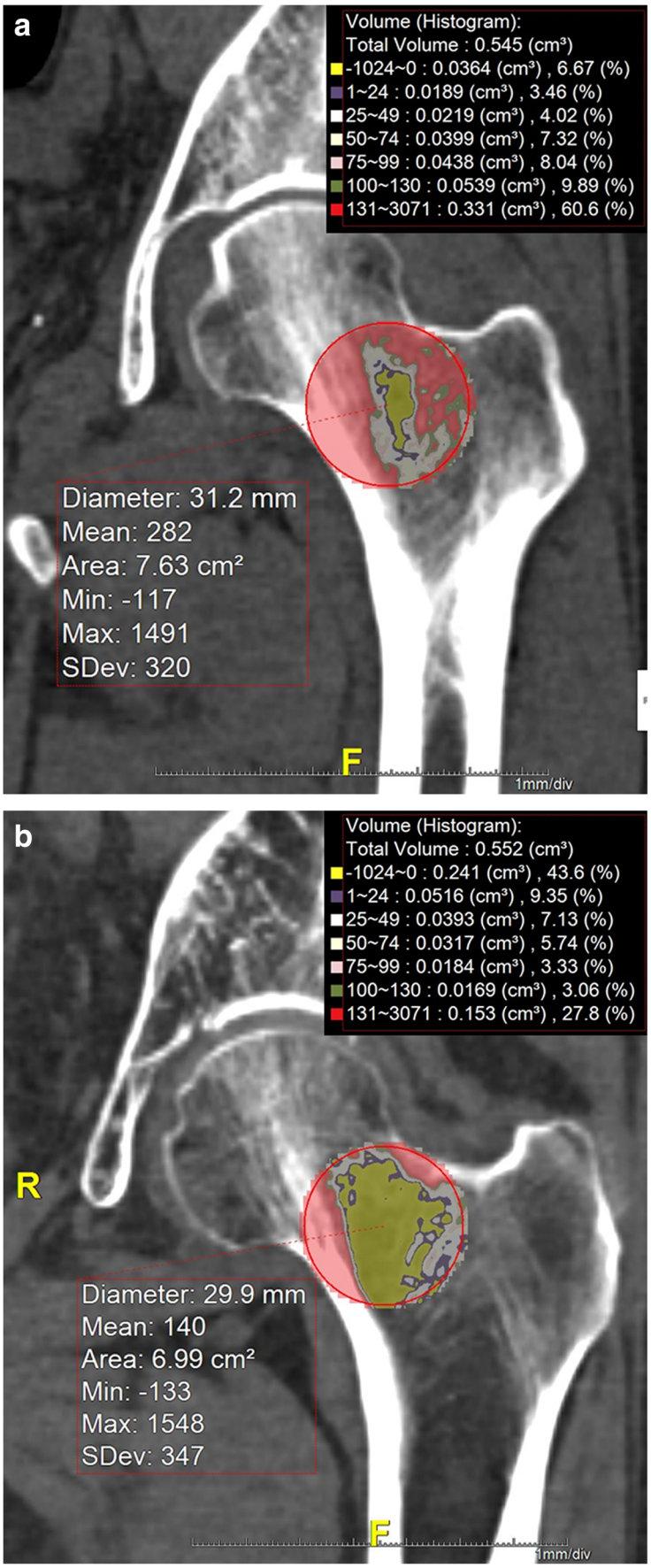

Fig. 2 Measurement of HUHA and average CT HU using the commercial 3-D analysis software (Aquarius iNtuition v4.4.12®). The ROI was drawn to include as much of Ward's triangle as possible. Images processed with HUHA analysis show (**a**) *T*-score -1.1 and (**b**) *T*-score -2.8

Table 1 Comparison of patient demographics and DXA, average CT HU, and HUHA values between the osteoporosis and non-osteoporosis groups

	Osteoporosis	Non-osteoporosis	*p*-value
Number	91	180	
Sex (M:F)	11:80	36:144	
Age, years	80.2 ± 9.4	64.1 ± 10.5	0.00
T-score	-3.3 ± 0.7	-0.9 ± 1.1	0.00
BMD (g/cm^2)	0.54 ± 0.82	0.83 ± 0.13	0.00
Interval from DXA to APCT (day)	4.7 ± 4.6	3.8 ± 6.8	0.31
Average CT HU	65.9 ± 55.1	209.1 ± 91.5	< 0.01
HUHA (% of ROI area)			
A (-1024 to 0 HU)	43.9 ± 12.2	15.5 ± 20.9	< 0.01
B (1–24 HU)	8.3 ± 2.3	6.4 ± 3.7	< 0.01
C (25–49 HU)	7.4 ± 2.3	7.1 ± 3.5	0.43
D (50–74 HU)	6.5 ± 2.2	7.7 ± 3.3	0.01
E (75–99 HU)	5.5 ± 1.9	7.8 ± 2.8	< 0.01
F (100–129 HU)	5.7 ± 5.9	8.8 ± 3.2	< 0.01
G (≥ 130 HU)	23.2 ± 9.3	47.7 ± 19.2	< 0.01

APCT abdominal-pelvic CT, *BMD* bone material density, *DXA* dual-energy X-ray absorptiometry, *HUHA* Hounsfield unit histogram analysis

Results

Patient descriptions

Patient demographics and DXA, HUHA, and average CT HU values are summarised in Table 1. The HUHA-A, HUHA-G, and average CT HU values are shown in Fig. 3. The prevalence of osteoporosis in this study cohort was 33.6%. A total of 178 patients underwent the 120 kVp CT protocol, and 93 patients underwent the 100 kVp CT protocol, but the average psoas muscle HU values at both tube voltages showed no significant difference (49.8 ± 5.1 vs. 49.5 ± 4.8, respectively; $p = 0.68$).

Correlation and simple linear regression analyses

HUHA-A showed a strong positive correlation with the presence of osteoporosis ($r = 0.74$, 95% confidence interval 0.69 to 0.79, $p < 0.01$), whereas the correlations of HUHA-G and the average CT HU with the femur *T*-score were moderate and negative ($r = -0.57$, 95% confidence interval -0.65 to -0.49, $p < 0.01$; $r = -0.64$, 95% confidence interval -0.71 and -0.57, $p < 0.01$, respectively). The correlations of the other HUHA categories were weakly positive or negative ($r = -0.33$ to 0.27). A significantly higher correlation with the *T*-score was obtained with HUHA-A than with either HUHA-G ($Z = 1.87$, $p = 0.03$) or the average CT HU ($Z = 1.89$, $p = 0.03$). Based on the correlation analysis, a simple linear regression equation was generated using HUHA-A (Fig. 4).

Diagnostic performance in predicting osteoporosis

According to the correlation analysis, diagnostic performance was evaluated using HUHA-A, HUHA-G, and the average CT HU. The diagnostic performance of each variable in predicting osteoporosis was assessed using ROC curves (Fig. 5). The area under the curve (AUC) for HUHA-A (0.95) showed a significant difference compared with those for HUHA-G (0.90) and the average CT HU (0.91; HUHA-A vs. HUHA-G, $p < 0.01$; HUHA-A vs. average CT HU, $p = 0.04$; HUHA-G vs. average CT HU, $p = 0.42$). Using the Youden index obtained from the ROC curve, the sensitivity and specificity in predicting osteoporosis were 95.6% and 81.7% for an HUHA-A cutoff value of ≥ 27.7%, 67.0% and 92.8% for a HUHA-G cutoff value of ≤ 31.6%, and 83.5% and 90.0% for an average CT HU cutoff value of ≤ 108, respectively. The negative predictive value of HUHA-A, HUHA-G, and the average CT HU was 97.3%, 84.7%, and 91.5%, respectively (Table 2).

Intra-observer and interobserver agreement

The ICCs between one observer's measurements and interobserver agreement are summarised in Table 3. The ICCs for HUHA-A, HUHA-G, and the average CT HU were good, and those of HUHA-A were almost perfect (kappa = 0.83). Substantial agreement was obtained for the interobserver validations of the other measurements.

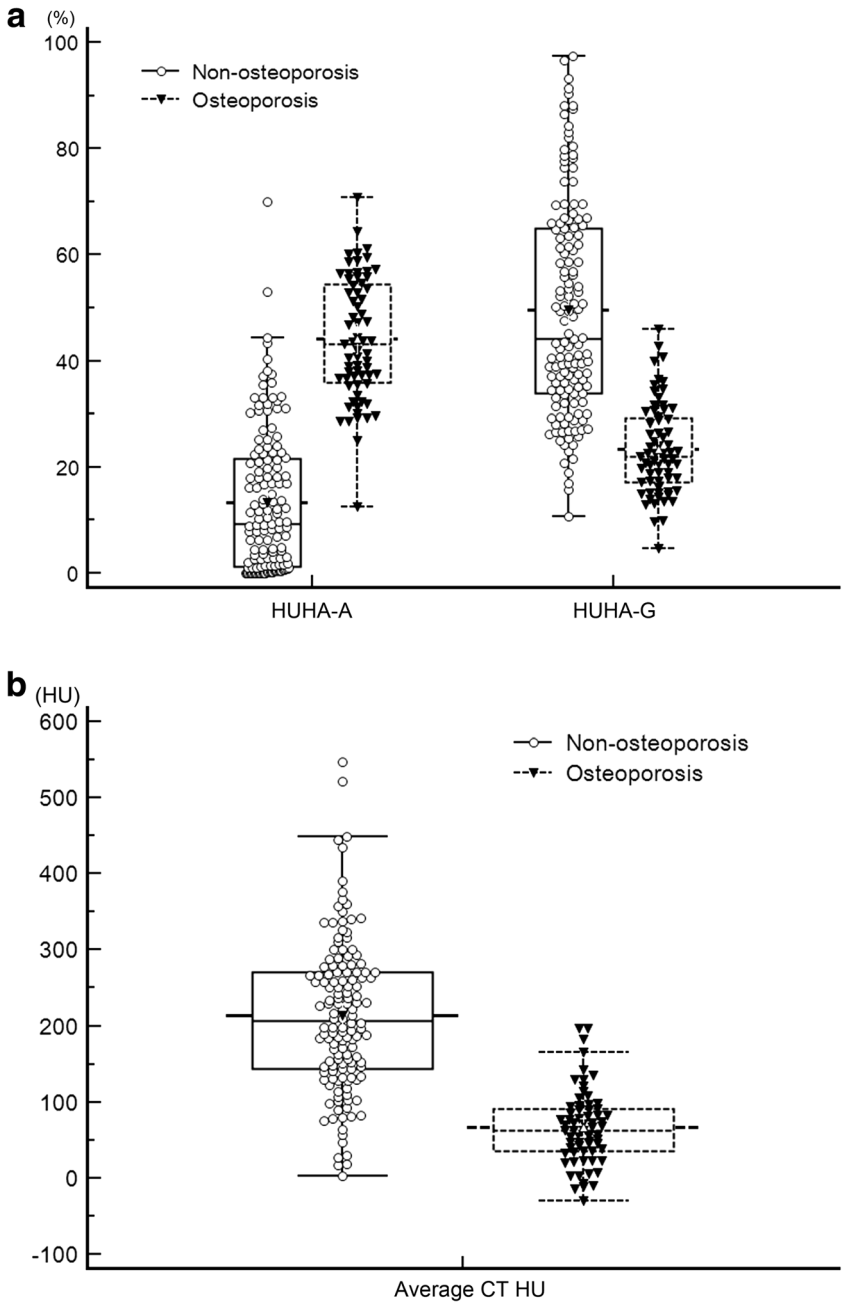

Fig. 3 Multiple comparison graphs of the HUHA-A, HUHA-G (**a**), and average CT HU (**b**) distribution between the osteoporosis and non-osteoporosis groups

Discussion

With the recent advances in 3-D image processing technology, CT image analysis has made it possible to analyse arbitrarily set CT HU range histogram as well as average CT HU value. In addition, several studies have shown that average CT HU values measured on lumbar spines or femoral neck are useful in diagnosing osteoporosis in either precontrast or post-contrast APCT [10, 12–14]. We hypothesised that histogram-range analysis of the CT HU would be more accurately reflect changes in the bony microstructure associated with osteoporosis as well as more useful in diagnosing osteoporosis than average CT HU value. In our study, we arbitrarily set up seven categories of HUHA. Among them, increase in HUHA-A (0 < HU), corresponding to the fatty marrow content in the femoral neck, showed strong positive correlation, and decrease in HUHA-G (≥ 130 HU), corresponding to the dense cortical bone content, showed moderate negative correlation with presence of the osteoporosis, respectively. Thus, our results reflected the pathophysiology of osteoporosis, in which the reduction in trabecular bony structure is replaced by fatty marrow, in addition to thinning of cortical bone during bone mineral loss [25, 26]. Especially, HUHA-A was strongly correlated with osteoporosis and may be used as

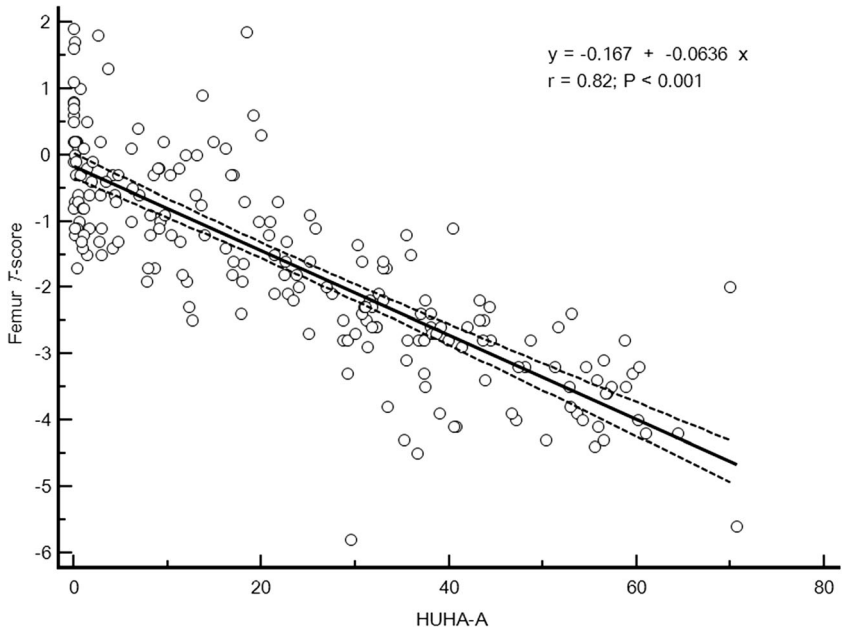

Fig. 4 Scatter plot and fitted linear regression line showing the relation between the femur *T*-score and HUHA-A, including the range for the estimated 95% prediction limit (dashed lines)

a semi-quantitative marker to evaluate cortical bone porosity and low BMD [26]. In our study, HUHA-A and HUHA-G showed not only a strong correlation with the pathophysiology of osteoporosis, but also a good diagnostic performance in the prediction of osteoporosis. Although all of HUHA-A, HUHA-G and average CT HU value showed good diagnostic performances (AUC > 0.9), HUHA-A showed significantly better diagnostic performance in predicting osteoporosis than did HUHA-G and the average CT HU value. Based on a HUHA-A cutoff value of ≥ 27.7%, deduced from the ROC analysis, HUHA-A showed a sensitivity of 95.6%, a specificity of 81.7%, and a negative predictive value of 97.3% in diagnosing osteoporosis. The corresponding each values for the average CT HU cutoff value of ≤ 108, deduced from the ROC analysis, were 83.5%, 90%, and 91.5%, respectively. Thus, our study showed that histogram analysis of CT HU in osteoporosis evaluation may be more useful than conventional image analysis based on measurement of the average CT HU value. The higher prevalence rate of the osteoporosis resulted in high sensitivities and negative predictive values of the screening tests. Although our results were from a single-centre retrospective study, HUHA-A, showed over 95% sensitivity and negative predictive value in diagnosing osteoporosis, could be a feasible method for opportunistic screening of osteoporosis in patients undergoing precontrast APCT.

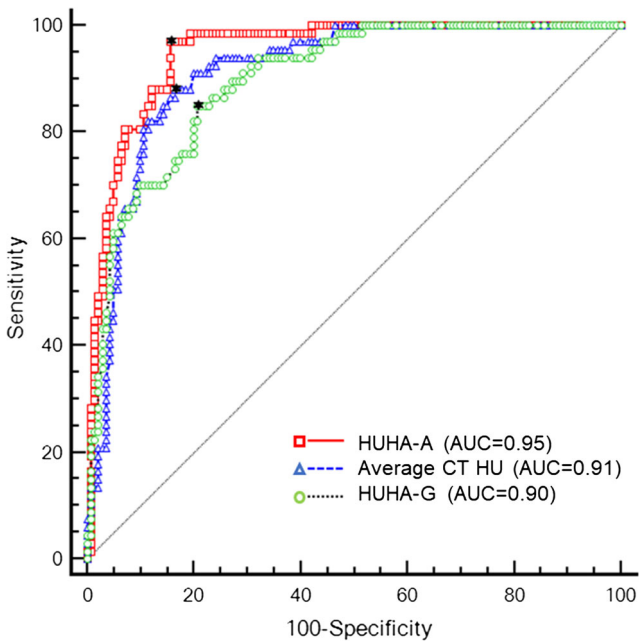

Fig. 5 Receiver operating characteristic curves predicting osteoporosis with HUHA-A (red box), HUHA-G (green circles), and average CT HU (blue triangle)

Pickhardt et al reported the diagnostic performance of the average CT HU value, which was associated with an AUC of ~ 0.83, sensitivity of 76%, and specificity of 75% at a 135 HU threshold for the lumbar spine [13]. Our results showed better AUC, sensitivity, and specificity for the diagnostic performance of the average CT HU value. The differences may be due to the following three factors. First, we measured the average CT HU at the femoral neck area instead of at the vertebral body, as the latter frequently undergoes degenerative change related to aging that may lead to an overestimation of BMD [27]. By contrast, the femoral neck is rarely affected by degenerative osteoarthritis [16]. Thus, the average CT HU of the femur more accurately reflects changes in osteoporosis than does the average CT HU of the lumbar spine. Second, because we used a low cutoff average CT HU value (108 HU), the sensitivity and specificity were higher. Third, compared

Table 2 Diagnostic accuracy of the HUHA-A, HUHA-G, and average CT HU values for osteoporosis (defined as a DXA femur T-score ≤ -2.5)

	Threshold	Sensitivity (%)	Specificity (%)	AUC (95% CI)	PPV (%)	NPV (%)
HUHA-A	≥ 27.7%	95.6	81.7	0.95 (0.91–0.98)	71.9	97.3
HUHA-G	≤ 31.6%	67.0	92.8	0.90 (0.85–0.94)	82.4	84.7
Average CT HU	≤ 108 HU	83.5	90.0	0.91 (0.87–0.95)	80.9	91.5

The prevalence of osteoporosis in the study cohort was 33.6%

AUC area under the curve, *DXA* dual-energy X-ray absorptiometry, *HUHA* Hounsfield unit histogram analysis, *PPV* positive predictive value, *NPV* negative predictive value

with other previous studies that focused on the lumbar spine and excluded cortical bone density, our ROI measurement included the outer margin of the cortical bone.

Our study design was similar to that of Gruber et al [28]. However, although the two studies are in agreement on the easy accessibility of the femur for HU measurement, with little technical effort and less time required, they have two major differences. First, Gruber et al measured the average HU value in axial images, whereas we measured the HU value range in coronal reformatted images. Second, because Gruber et al used contrast-enhanced CT images, additional phantom imaging and a HU value correction process were required. Nonetheless, both our study (r = 0.74) and that of Gruber et al (r = 0.79 - 0.84) found a strong correlation with the DXA results in predicting osteoporosis of the femoral neck. Thus, these studies demonstrate the feasibility of osteoporosis screening based on measurements of HU value on either precontrast or contrast-enhanced APCT of the femur, regardless of whether the images are axial or coronal or whether contrast medium is used in the examination.

The HUHA method has the following advantages. First, it is easy to perform and shows high repeatability. The observer does not require special training, knowledge, or experience to select and draw a ROI. Rather, the observer selects the best image of Ward's triangle containing the largest amount of fatty marrow and then draws the largest ROI on the femoral neck, including as much of Ward's triangle as possible. Although there was no specific interactive training session before HUHA measurements were made, intra- and interobserver agreement was either good or substantial. In addition, HUHA measurements do not require a significant amount of time when performed in daily routine clinical practice. The commercial 3-D program can be linked to the PACS, and patient images that require analysis in real time can be retrieved. The time required to analyse one image was about 1 min. However, as far as we know, Aquarius iNtuition® is the only commercial program that allows a histogram analysis of the CT number of a specific region. Second, this method provides colour-overlay CT images depicting the extent of bone mineral loss; thus, intuitive estimates of osteoporosis are possible. Third, semi-quantitation of the change in bone mineral loss is possible. We divided the HU range into seven arbitrarily chosen intervals, but the HU range can be set by the user. Fourth, unlike with quantitative CT or quantitative ultrasound CT, additional equipment, phantom, or daily practice is not required [29]. Measurement of HU values is significantly affected by the intravenous contrast medium. Pompe et al showed that injection of contrast medium substantially increases the HU value compared with precontrast CT and thus leads to an underestimation of osteoporosis [21]. Gruber et al showed that the BMD values obtained from contrast-enhanced CT images of the femoral neck correlate strongly with the DXA reference value but that a special conversion process is required for the determination [28]. To avoid this effect of contrast medium, we measured HUHA and the mean CT HU on precontrast CT scan images. However, both measurements are affected not only by the use of an intravenous contrast medium and a reduction in the radiation dose, such as achieved with automated tube current selection and a projection angle with iterative reconstruction but also by scanner instability; the presence of fat within the bone marrow; and, in single-energy CT, beam hardening artefacts, patient scatter, and metal artefacts [9, 30]. Mei K et al reported bone mineral density showed no significant change regardless of sparse sampling and low tube current. But, quantitative trabecular bone microstructure measurement was sensitive to dose reduction [30]. In our study we observed a strong positive correlation between HUHA-A and osteoporosis prediction.

Table 3 Intra-observer and inter-observer agreement of HUHA and average CT HU measurement

	HUHA-A (95% CI)	HUHA-G (95% CI)	Average CT HU (95% CI)
Intra-observer agreement (ICC)	0.96 (0.85, 0.99)	0.92 (0.79, 0.97)	0.92 (0.84, 0.96)
Inter-observer agreement (Kappa)	0.83 (0.77, 0.89)	0.60 (0.45, 0.76)	0.73 (0.63, 0.83)

ICC a two-way mixed intra-class correlation coefficient with absolute agreement

95% CI 95% confidence interval

Because our study was performed on single-energy precontrast APCT using either 100 kVp or 120 kVp tube voltage, the HUHA value may vary slightly depending on the CT protocol.

DECT can be a suitable alternative to solve these problems. Compared with single-energy CT, dual-energy CT enables reducing beam hardening artefacts and metal artefacts, more precise tissue characterisation based on the calculation of the effective atomic number and electron density of substances and showed strong linear correlation regardless of tube voltage [9, 31–33]. With these advantages, dual-energy CT had a strong advantage with measurement of marrow fat tissue content, quantitative analysis of bony microstructure, and bone mineral density [31–33]. A more sophisticated analysis of bone composition can be achieved when HUHA is combined with a bone density calibration phantom and dual-energy CT scan. It may also help to quantitatively evaluate the effect of therapeutic agents on osteoporosis. Additional studies are needed to more fully evaluate the potential effects of the HUHA according to the various scan strategies of single-energy or dual-energy CT.

Our study has some limitations. First, this was a retrospective single-centre study. There was a potential for selection bias associated with the retrospective inclusion of patients. We enrolled patients older than 50 years who underwent DXA as a standard reference test. DXA is recommended to a woman age 65 or older, a man age 70 or older, bony fracture after age 50, menopause age with risk factors, postmenopausal woman under age 65 with risk factors and man age 50–69 with risk factors [34, 35]. In addition, the Fracture Risk Assessment Tool (FRAX) is another test used in conjunction with DXA for the osteoporosis screening among younger postmenopausal women aged 50–64 years, but it requires the results of the DXA [36, 37]. The purpose of our study was to evaluate the usefulness of the diagnosis and opportunistic screening of osteoporosis using precontrast APCT, by referring to these references, we limited the age of the patients to 50 years of age or older. Second, there were many patients with breast cancer. Although 157 patients undergoing tumour metastasis surveillance were included in this study, none had received chemotherapy before the test, and the duration of DXA and APCT was limited to 1 month or less. Thus, changes in BMD related to chemotherapy were presumably negligible. Third, the seven HU range categories were selected arbitrarily. Each HUHA range was arbitrarily set because it was the first trial to be attempted. However, HUHA-A and HUHA-G assumed fatty marrow content and dense cortical bone, respectively, referring to the results of previous studies [13, 17]. Thresholds and diagnostic performances are study-dependent and require a larger cohort and external validation. Fourth, although our CT machines are regularly calibrated according to the manufacturer's guidelines, the HU values may have differed based on X-ray beam properties. Although there was no significant difference in the HU of the psoas muscle according to the tube voltages, there is an inevitable difference in the HU value depending on the CT device and the protocol used.

In conclusion, our study showed that HUHA measurements in the femoral neck are closely related to BMD and can be used to predict osteoporosis as defined by the DXA *T*-score. Among the HUHA-A, HUHA-G, and average CT HU values, a HUHA-A cutoff value of ≥ 27.7% showed the best diagnostic performance in predicting osteoporosis, with 95.6% sensitivity and 81.7% specificity.

Funding The authors state that this work has not received any funding.

Compliance with ethical standards

Guarantor The scientific guarantor of this publication is Kwanseop Lee.

Conflict of interest The authors of this manuscript declare no relationships with any companies, whose products or services may be related to the subject matter of the article.

Statistics and biometry No complex statistical methods were necessary for this paper.

Informed consent Written informed consent was waived by the Institutional Review Board.

Ethical approval Institutional Review Board approval was obtained.

Methodology
- retrospective
- diagnostic or prognostic study
- performed at one institution

References

1. Sambrook P, Cooper C (2006) Osteoporosis. Lancet 367:2010–2018
2. Riggs BL, Melton LJ 3rd (1995) The worldwide problem of osteoporosis: Insights afforded by epidemiology. Bone 17:505S–511S
3. Office of the Surgeon General (US) (2004) Bone Health and Osteoporosis: A Report of the Surgeon General. Office of the Surgeon General (US), Rockville (MD) Available from: https://www.ncbi.nlm.nih.gov/books/NBK45513/. Accessed 17 Aug 2018
4. Johnell O, Kanis JA, Odén A et al (2004) Mortality after osteoporotic fractures. Osteoporos Int 15:38–42
5. Lewiecki EM, Gordon CM, Baim S et al (2008) International Society for Clinical Densitometry 2007 adult and pediatric official positions. Bone 43:1115–1121
6. Nelson HD, Haney EM, Dana T, Bougatsos C, Chou R (2010) Screening for osteoporosis: An update for the US. Preventive Services Task Force. Ann Intern Med 153:99–111
7. Amarnath AL, Franks P, Robbins JA, Xing G, Fenton JJ (2015) Underuse and overuse of osteoporosis screening in a regional health system: a retrospective cohort study. J Gen Intern Med 30:1733–1740
8. Gillespie CW, Morin PE (2017) Osteoporosis-related health services utilization following first hip fracture among a cohort of

privately-insured women in the United States, 2008-2014: an observational study. J Bone Miner Res 32:1052–1061
9. van Hamersvelt RW, Schilham AM, Engelke K et al (2017) Accuracy of bone mineral density quantification using dual-layer spectral detector CT: A phantom study. Eur Radiol 27:4351–4359
10. Pompe E, de Jong PA, de Jong WU et al (2016) Inter-observer and inter-examination variability of manual vertebral bone attenuation measurement on computed tomography. Eur Radiol 26:3046–3053
11. Emohare O, Cagan A, Morgan R et al (2014) The use of computed tomography attenuation to evaluate osteoporosis following acute fractures of the thoracic and lumbar vertebra. Geriatr Orthop Surg Rehabil 5:50–55
12. Tay WL, Chui CK, Ong SH, Ng AC (2012) Osteoporosis screening using areal bone mineral density estimation from diagnostic CT images. Acad Radiol 19:1273–1282
13. Pickhardt PJ, Lee LJ, del Rio AM et al (2011) Simultaneous screening for osteoporosis at CT colonography: Bone mineral density assessment using MDCT attenuation techniques compared with the DXA reference standard. J Bone Miner Res 26:2194–2203
14. Mueller DK, Kutscherenko A, Bartel H, Vlassenbroek A, Ourednicek P, Erckenbrecht J (2011) Phantom-less QCT BMD system as screening tool for osteoporosis without additional radiation. Eur J Radiol 79:375–381
15. Buckens CF, Dijkhuis G, de Keizer B, Verhaar HJ, de Jong PA (2015) Opportunistic screening for osteoporosis on routine computed tomography? An external validation study. Eur Radiol 25:2074–2079
16. Liu G, Peacock M, Eilam O, Dorulla G, Braunstein E, Johnston CC (1997) Effect of osteoarthritis in the lumbar spine and hip on bone mineral density and diagnosis of osteoporosis in elderly men and women. Osteoporos Int 7:564–569
17. Poole KES, Skingle L, Gee AH et al (2017) Focal osteoporosis defects play a key role in hip fracture. Bone 94:124–134
18. Fujii M, Aoki T, Okada Y et al (2016) Prediction of femoral neck strength in patients with diabetes mellitus with trabecular bone analysis and tomosynthesis images. Radiology 281:933–939
19. Kanis JA (2002) Diagnosis of osteoporosis and assessment of fracture risk. Lancet 359:1929–1936
20. Johnell O, Kanis JA, Odén A et al (2005) Predictive value of BMD for hip and other fractures. J Bone Miner Res 20:1185–1194
21. Pompe E, Willemink MJ, Dijkhuis GR, Verhaar HJ, Mohamed Hoesein FA, de Jong PA (2015) Intravenous contrast injection significantly affects bone mineral density measured on CT. Eur Radiol 25:283–289
22. Shrout PE, Fleiss JL (1979) Intraclass correlations: Uses in assessing rater reliability. Psychol Bull 86:420–428
23. Büsing KA, Kilian AK, Schaible T, Debus A, Weiss C, Neff KW (2008) Reliability and validity of MR image lung volume measurement in fetuses with congenital diaphragmatic hernia and in vitro lung models. Radiology 246:553–561
24. Landis JR, Koch GG (1977) An application of hierarchical kappa-type statistics in the assessment of majority agreement among multiple observers. Biometrics 33:363–374
25. Chen H, Zhou X, Fujita H, Onozuka M, Kubo KY (2013) Age-related changes in trabecular and cortical bone microstructure. Int J Endocrinol 2013:213234
26. Sundh D, Rudang R, Zoulakis M, Nilsson AG, Darelid A, Lorentzon M (2016) A high amount of local adipose tissue is associated with high cortical porosity and low bone material strength in older women. J Bone Miner Res 31:749–757
27. Yu W, Glüer CC, Fuerst T et al (1995) Influence of degenerative joint disease on spinal bone mineral measurements in postmenopausal women. Calcif Tissue Int 57:169–174
28. Gruber M, Bauer JS, Dobritz M et al (2013) Bone mineral density measurements of the proximal femur from routine contrast-enhanced MDCT data sets correlate with dual-energy X-ray absorptiometry. Eur Radiol 23:505–512
29. Link TM (2012) Osteoporosis imaging: State of the art and advanced imaging. Radiology 263:3–17
30. Mei K, Kopp FK, Bippus R et al (2017) Is multidetector CT-based bone mineral density and quantitative bone microstructure assessment at the spine still feasible using ultra-low tube current and sparse sampling? Eur Radiol 27:5261–5271
31. Wichmann JL, Booz C, Wesarg S et al (2015) Quantitative dual-energy CT for phantomless evaluation of cancellous bone mineral density of the vertebral pedicle: Correlation with pedicle screw pull-out strength. Eur Radiol 25:1714–1720
32. Wichmann JL, Booz C, Wesarg S et al (2014) Dual-energy CT-based phantomless in vivo three-dimensional bone mineral density assessment of the lumbar spine. Radiology 271:778–784
33. Booz C, Hofmann PC, Sedlmair M et al (2017) Evaluation of bone mineral density of the lumbar spine using a novel phantomless dual-energy CT post-processing algorithm in comparison with dual-energy X-ray absorptiometry. Eur Radiol Exp 1:11. https://doi.org/10.1186/s41747-017-0017-2
34. US Preventive Services Task Force (2011) Screening for osteoporosis: U.S. preventive services task force recommendation statement. Ann Intern Med 154:356–364
35. Lim LS, Hoeksema LJ, Sherin K, ACPM Prevention Practice Committee (2009) Screening for osteoporosis in the adult U.S. population: ACPM position statement on preventive practice. Am J Prev Med 36:366–375
36. Crandall CJ, Larson J, Gourlay ML et al (2014) Osteoporosis screening in postmenopausal women 50 to 64 years old: comparison of US Preventive Services Task Force strategy and two traditional strategies in the Women's Health Initiative. J Bone Miner Res 29:1661–1666
37. Kanis JA, Johnell O, Oden A, Johansson H, McCloskey E (2008) FRAX and the assessment of fracture probability in men and women from the UK. Osteoporos Int 19:385–397